

Shear velocity structure of the Hellenic upper mantle from Rayleigh-wave dispersion

I. Kassaras, V. Kapetanidis, I. Spingos, A. Karakonstantis, G. Kaviris, P. Papadimitriou

Department of Geophysics & Geothermics, NKUA, Panepistimiopolis, 15784 Athens, Greece, kassaras@geol.uoa.gr

The dynamics of the Hellenic lithosphere has been extensively studied over the last decades. However, tomographic investigations on the seismic structure of its upper mantle have yielded controversial interpretations, mostly related to restraints due to poor resolution, especially for the intermediate depth range down to 150 km. This study provides new constraints on the intermediate depth, upper-mantle shear velocity structure of Greece using broadband Rayleigh-wave recordings. The analysis is a three-step procedure: acquisition of waveform recordings, dispersion curve estimation, and inversion. The data are constituted of broadband waveforms of over 670 events recorded by ~200 broadband stations of the Hellenic Unified Seismological Network (HUSN; <http://www.gein.noa.gr/en/networks/husn>) and Kandilli Observatory and Earthquake Research Institute network (KOERI, 2001) between 2010 and 2018. Additional recordings were acquired from stations of the Corinth Rift Laboratory (CRL), operating in Central Greece, as well as of GEOFON and MEDNET.

Phase-velocity dispersion curves were derived using a multichannel cross-correlation technique, applying the Automated Surface-Wave Measuring System algorithm (ASWMS; Jin and Gaherty, 2015), based on the Generalized Seismological Data Functionals (GSDF) proposed by Gee & Jordan (1992). In this method, phase delays are measured between all combinations of neighboring stations of the network to avoid systematic biases due to propagation effects, rather than only for pairs that are aligned with the epicenter, within a few degrees of tolerance along a common great circle path; an assumption that greatly reduces the number of quasi-valid measurements. Phase-velocities were determined in terms of apparent and structural velocities, approximated by the application of the Eikonal and Helmholtz equation, respectively. Phase-velocity maps were generated in a grid cell of cell-dimensions $0.2^\circ \times 0.2^\circ$ over the period range 30 to 90 s (Fig. 1a). Checkerboard tests yielded adequate horizontal resolution to distinguish anomalies of about $130 \times 130 \text{ km}^2$ for the obtained tomograms.

The phase-velocity maps were then inverted in order to acquire the vertically polarized shear-velocity (V_{SV}) distribution with depth, using the *surf96* code (Herrmann, 1994), derived by a Monte-Carlo scheme on perturbations over initial 1-D models, as implemented in the ASWSM suite (Jin, 2015), modified to take into account the region's crustal structure (CRUST1.0; Laske *et al.*, 2013). The most prevalent features in the phase velocity maps (Fig. 1) are the Hellenic Subduction Zone (HSZ) and the North Anatolia Trench system (NAT), manifested by high and low velocities, respectively. Low velocities along the outer Hellenic Arc at low periods are pertinent to the thick crust and sedimentation along the HSZ (Laske *et al.*, 2013). Fast velocities beneath the Cephalonia-Lefkas-Akarnania Block (CLAB, Fig. 1), considered a microplate (Perouse *et al.*, 2017) are indicative for deep lithospheric roots. A high velocity anomaly extends below the Greek mainland and the South Aegean Active Volcanic Arc (SAAVA), consistently with other tomographic studies (e.g. Papazachos & Nolet, 1997).

Cross-sections across the 3-D absolute V_{SV} model (Fig. 2) highlight a low velocity zone hosting intermediate depth seismicity, above a high velocity surrounding upper mantle material deeper than 90 km. This finding is compatible with Spakman and Nolet (1988) and Granet and Trampert (1989), who interpreted a low velocity anomaly at similar depth as representing a possible detachment zone along the slab, and with Suckale *et al.* (2009) who found a low-velocity layer at the western part of the HSZ at depths 40-90 km, explained as the hydrated crust of the Hellenic slab. The upper mantle of North Aegean is dominated by slow velocities, compatible with mantle wedge, asthenospheric flow and surface magmatism observed throughout the region. The latter observation, also complies with high crustal stress ratio values (Kapetanidis and Kassaras, 2019), indicative of a stable S_3 axis, exhibiting extension in a SSW-NNE direction.

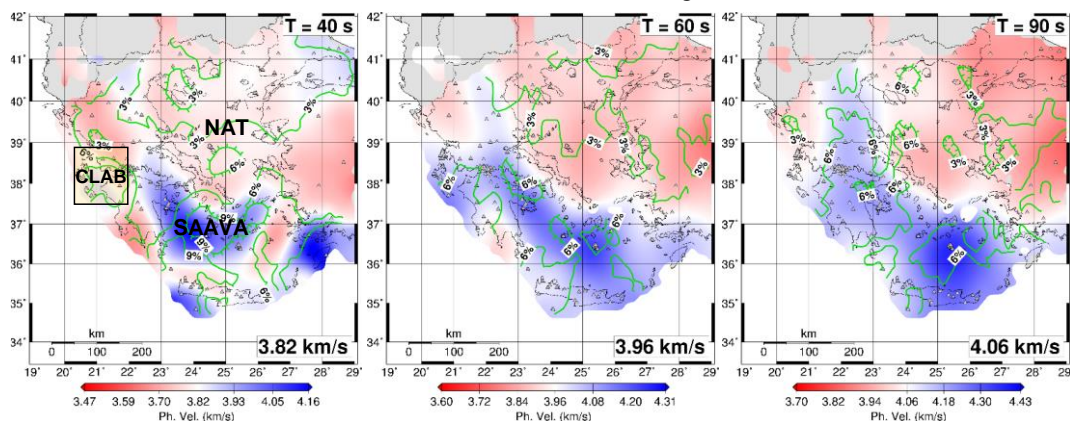


Figure 1. Rayleigh-wave structural (Helmholtz) phase velocity maps at various periods of interest. The color scale varies with period T, with white color corresponding to the average phase velocity as given in the lower right corner of each map. Green contours indicate relative error (%) with respect to the average phase velocity per period. Tick lines on the contours indicate the direction of relative error reduction.

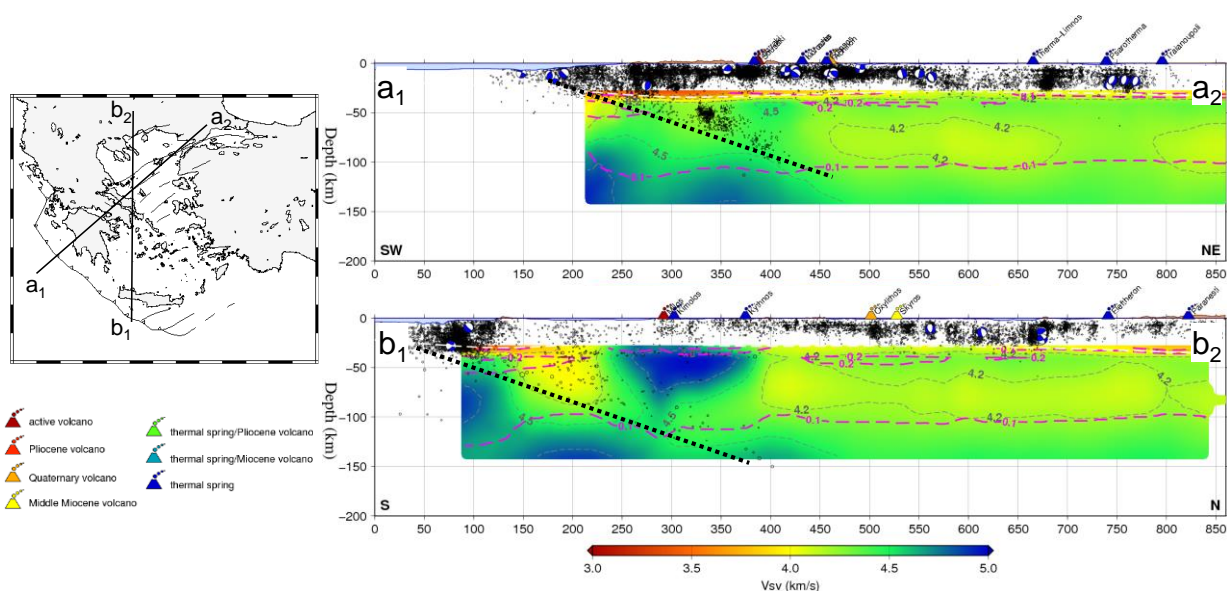


Figure 2. Cross sections of preliminary results on the 3-D absolute V_{sv} model along profiles shown on the left map. Purple dashed lines are contours of the Resolution matrix Diagonal Element (RDE), with results in regions within $RDE > 0.1$ generally considered as reliable. Seismicity (Karakonstantis, 2017; Bocchini, 2018), focal mechanisms (Kapetanidis & Kassaras, 2019) and volcanics (Siebert & Simkin, 2002) are superimposed.

Acknowledgements

We acknowledge support of this study by the project “HELPOS - Hellenic Plate Observing System” (MIS 5002697) which is implemented under the Action “Reinforcement of the Research and Innovation Infrastructure”, funded by the Operational Programme “Competitiveness, Entrepreneurship and Innovation” (NSRF 2014-2020) and co-financed by Greece and the European Union (European Regional Development Fund). We thank EIDA for providing data from regional networks HL (doi: 10.7914/SN/HL), HT (doi: 10.7914/SN/HT), HA (doi: 10.7914/SN/HA), HP (doi: 10.7914/SN/HP), HC (doi: 10.7914/SN/HC), CQ (doi:10.7914/SN/CQ), Z3 (doi:10.14470/M87550267382), and CL (doi:10.15778/RESIF.CL). We are greatly indebted to Ge Jin, Natalie Accardo for clarifications on the ASWSM suite and A. Ganas for discussions.

References

- Bocchini, G.M., 2018. Big or Small Earthquakes along the Subduction Interface: Impact on Natural Hazards, PhD Thesis, National and Kapodistrian University of Athens, p.249.
- Gee, L.S. & Jordan, T.H., 1992. Generalized seismological data functionals, *Geophys. J. Int.*, 111(2), 363–390.
- Granet, M. And Trampert, J., 1989. Large scale P-velocity structures in the EuroMediterranean area, *Geophysical Journal International*, 99, 583–594.
- Herrmann, R.B., 1994. Computer programs in Seismology, User’s manual. St. Louis University, Missouri.
- Jin, G. & Gaherty, J.B., 2015. Surface wave phase-velocity tomography based on multichannel cross-correlation, *Geophys. J. Int.* (2015) 201, 1383–1398, doi: 10.1093/gji/ggv079.
- Jin, G., 2015. Surface-wave analysis and its application to determining crustal and mantle structure beneath regional arrays, PhD Thesis, Columbia University, USA, pp. 126.
- Kapetanidis, V., Kassaras, I., 2019. Contemporary crustal stress of the Greek region deduced from earthquake focal mechanisms, *J. of Geodynamics*, DOI: 10.1016/j.jog.2018.11.004.
- Karakonstantis, A., 2017. 3-D simulation of crust and upper mantle structure in the broader Hellenic area through Seismic Tomography, PhD Thesis, National and Kapodistrian University of Athens, (in Greek).
- KOERI, 2001. Bogazici University Kandilli Observatory and Earthquake Research Institute. International Federation of Digital Seismograph Networks. Other/Seismic Network. 10.7914/SN/KO, <https://doi.org/10.7914/SN/KO>
- Laske, G., Masters, G., Ma, Z. and Pasyanos, M., 2013. Update on CRUST1.0 - A 1-degree Global Model of Earth's Crust, *Geophys. Res. Abstracts*, 15, Abstract EGU2013-2658.
- Papazachos, C.B., Nolet, G. 1997. P and S deep structure of the Hellenic area obtained by robust nonlinear inversion of travel times. *Journal of Geophysical Research*, 102, 8349–8367.
- Pérouse E., et al., 2017. Transition from collision to subduction in Western Greece: The Katouna-Stamna active fault system, *Int. J. Earth Sci.*, 106, 967-989.
- Siebert, L., Simkin, T., 2002–present. *Volcanoes of the World: an Illustrated Catalog of Holocene Volcanoes and their Eruptions*. Smithsonian Institution, Global Volcanism Program Digital Information Series, GVP-3 (<http://www.volcano.si.edu>).
- Spakman, W., Nolet, G. (1988). Imaging algorithms, accuracy and resolution in delay time tomography. In N.J. Vlaar, G. Nolet, M.J.R. Wortel, & S.A.P. Cloetingh (Eds.), *Mathematical geophysics: A survey of recent developments in seismology and geodynamics* (pp. 155–187). Netherlands: Springer.
- Suckale, J., et al., 2009. High-resolution seismic imaging of the western Hellenic subduction zone using teleseismic scattered waves, *Geophys. J. Int.*, 178, 775–791, doi: 10.1111/j.1365-246X.2009.04170.x.